Demonstration of 80-Gbps Long-haul MMW SIMO Delivery Employing MIMO CMA and MRC Technology

Weiping Li(1), Jianjun Yu (1)*, Xianmin Zhao(2), Jiaxuan Liu(1), Yi Wei(1), Tianqi Zheng(1), Mingxu Wang(1), Xiongwei Yang(1), Kaihui Wang(1), Wen Zhou(1), Bo Liu(1), and Feng Zhao(3)

(1) Fudan University, Shanghai, 200433, China * jianjun@fudan.edu.cn
(2) Harbin Institute of Technology, Harbin, China, 150001
(3) Xi'an University of Posts and Telecommunications, Xi'an, 710121, China

Abstract: A joint MIMO CMA and MRC receiving technology is proposed and experimentally verified in a photonics-aided long-haul SIMO MMW delivery system, which can achieve up to 80-Gbps 16QAM signal delivery over 4600 m wireless distance. *©2023 The Authors*

Introduction

Photonics-aided technology has been applied in millimeter-wave (MMW, 30-300GHz) communication systems to effectively resist the bandwidth limitation and electromagnetic interference of electronic equipment, which can also effectively promote the seamless integration of wireless and fiber-optic networks [1-5]. However, the photonics-aided long-haul MMW transmission systems usually suffer from low received power and poor signal-to-noise ratio (SNR) at the wireless receiver due to the efficiency limitation of the photo-electric (O-E) conversion transmitter using photomixing and the characteristics of weak penetration and strong atmospheric attenuation at MMW band [6].

Due to the contradiction between SNR and communication capacity, single-antenna technology is difficult to achieve satisfactory performance [7-9]. Based on single-antenna technology, Kanno *et al.* have achieved 20-Gbps QPSK MMW wireless transmission in free space with a distance of 30 mm [7], and Puerta *et al.* have achieved 60-Gbps single side-band multi-band CAP transmission over 2.13 m air distance [9]. Recently, we have experimentally demonstrated 47.5-Gbps and 23.1-Gbps multi-carrier delivery at W-band (75-110GHz) and D-band (110-170GHz), respectively, over 4.6 km free space employing advanced DSP and optoelectronic equipment [10-11].

In this paper, we employ a space diversity-based multi-antenna technology for a photonics-aided MMW delivery system, which can indirectly moderate the contradictions of SNR and data rate. For the first time, we propose and adopt a joint multiple-input and multiple-output ((MIMO) constant-modulus-algorithm (CMA) and maximum ratio combination (MRC) receiving technology to improve the SNR of our receivers so that the transmission system can support higher data rate. As a result of outdoor field experimental verification, the 80-Gbps 16QAM signal delivery demonstration based on a photonics-aided single-input multiple-output (SIMO) MMW system over 4600 m wireless distance has been successfully carried out.

The principle of MIMO CMA and MRC

In a single-antenna system, channel impairments may occur during transmission. In this case, CMA, as a blind adaptive algorithm for adaptive filter coefficients, can be used to compensate for these impairments [12]. The CMA estimates the channel impulse response and can be used at the receiver to eliminate channel interference. In addition, as what has been done in the fiber-wireless MIMO communication [13], a CMA-based four-butterfly configured adaptive digital equalizers, called MIMO CMA, whose structure is shown in Fig.1(a), can be used for both polarization and wireless MIMO demultiplexing [14]. However, the four-butterfly MIMO CMA as a linear equalization, can also realize the dynamic channel equalization and correct the linear damages of the multi-channel system. The tap weight update equation for MIMO CMA is as follows:

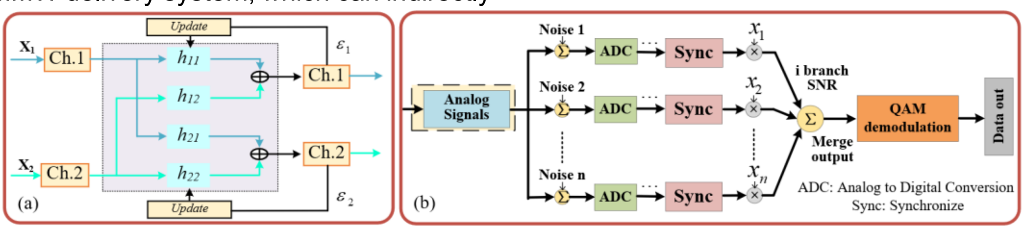

Fig.1: (a) The structure of MIMO CMA; (b) The principle of the MRC technology

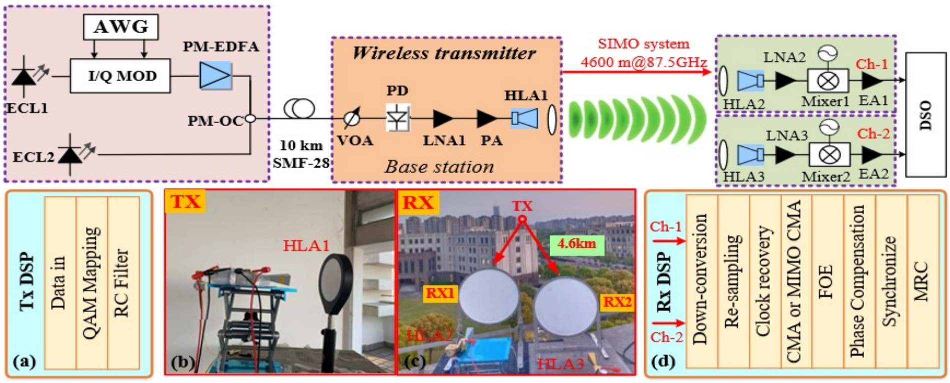

Fig.2: The experimental setup of the photonics-aided long-haul MMW SIMO delivery system; (a) Block diagram of Tx DSP; (b) The experimental photos at TX-end; (c) The experimental photos at RX-end (Tx and Rx are located between the two campuses of Fudan University); (d) Block diagram of Rx DSP.

$$h_{11} = h_{11} + \mu\varepsilon_1 e_1(i) X_1^*(i-k)$$
$$h_{12} = h_{12} + \mu\varepsilon_1 e_1(i) X_2^*(i-k)$$
$$h_{21} = h_{21} + \mu\varepsilon_2 e_2(i) X_1^*(i-k)$$
$$h_{22} = h_{22} + \mu\varepsilon_2 e_2(i) X_2^*(i-k)$$

In a space diversity system based on multi-antenna, multiple-channel signals can be included in the MIMO CMA process to obtain a more accurate estimate of the channel impulse response, which can effectively improve system performance by compensating for channel impairments and improving signal quality.

In addition, it is possible to get the output signals with maximum SNR utilizing MRC technology in a space diversity system based on multi-antenna [15]. The principle of the MRC technology is demonstrated in Fig.1(b). Assuming that the noise power density is represented by N_0, and the SNR of the n-th branch is denoted by $\gamma_n = \alpha_n^2 E_s / N_0$, the MRC process involves the determination of the weighting coefficient for each branch, represented by x_n, n = 1, 2,…,N_r. After applying the weighting coefficients, the amplitude of the signals in equivalent baseband received by the n-th branch is $x_n \alpha_n \sqrt{E_s}$. However, the noise power in this branch is also amplified by a factor of x_n^2. After adjusting each branch to the same phase and adding the signals together, we obtain an integrated signal with a corresponding amplitude, represented by $\sum_{n=1}^{N_r} \alpha_n x_n \sqrt{E_s}$. The SNR of the integrated signals is

$$\gamma\left(x_1, x_2, \ldots, x_{N_r}\right) = \frac{\left(\sum_{n=1}^{N_r} \alpha_n x_n \sqrt{E_s}\right)^2}{\sum_{n=1}^{N_r} x_n^2 N_0} = \frac{E_s}{N_0} \frac{\left(\sum_{n=1}^{N_r} \alpha_n x_n\right)^2}{\sum_{n=1}^{N_r} x_n^2}$$

To find the maximum SNR in the MRC process, we need to optimize the weighting coefficient of each branch. This is an extremum problem of a function of several variables, which requires finding the extreme point that satisfies certain conditions. Specifically, the extreme point should satisfy the following condition:

$$\frac{x_i}{x_j} = \frac{\alpha_i}{\alpha_j}, i, j = 1, \ldots, N_r, i \neq j$$

With this information, we can adjust the weighting coefficients in each branch accordingly to achieve the best possible signal quality for the integrated signals.

Experimental setup

The setup used for the high-speed long-haul mm-wave wireless transmission system is illustrated in Fig.2. Continuous waves of 1550 nm and 1550.7 nm are emitted by two free-running external cavity lasers (ECL1 and ECL2) with a linewidth of less than 100kHz and a typical frequency stability of ±0.3 GHz for 24 hours. The I/Q modulator (3dB bandwidth of 40 GHz), is driven by the 13 dBm CWs emitted from ECL1. In the Tx-side, an 120-Gsa/s arbitrary waveform generator(AWG) transfroms the digital QAM signals filtered by a raised-cosine (RC) filter with a 0.01 roll-off factor to anglog signals. The RC filter is used to resist the bandwidth limitation of photoelectric devices. After being generated by the AWG, the I-th and Q-th analog electrical signals undergo amplification through a pair of parallel electric amplifiers (EAs) with a 25 dB gain. These amplified signals are then fed into the I/Q modulator for modulation. A PM-OC couple the 10 dbm CWs, emitted from ECL2, with the optical signals, which is amplified by a PM-EDFA to compensate for the insertion loss of the modulator. Once the optical signals have traversed the 10 km length of SMF-28 fiber, they are directed through a variable optical attenuator (VOA). Then the 87.5 GHz mm-wave signals are generated via a photodiode (PD) with 3-dB bandwidth of 100 GHz. The MMW signals are boosted by a low noise amplifier (LNA1) and W-band power amplifier (PA) successively, and then they are transmitted by a horn lens antenna (HLA1). After 4600 m wireless transmission, the MMW signals reach the receiving end, which is composed of two independent wireless receivers. The experimental photos at TX-end and RX-end are shown in Fig.2(b-c), respectively. In the wireless receivers, the MMW signals are first received by lens horn antennas (HLA2 and HLA3), boosted by low noise amplifiers (LNA2 and LNA3), and then down-converted to 12.5 GHz intermediate frequency (IF) signals by mixers driven by 75GHz radio frequency (RF) signals. We use two EAs (EA1 and EA2) to enhance the IF signals and finally use a digital storage oscilloscope (DSO) to capture the enhanced IF signals. The DSP process at RX-end shown in Fig.2(d) includes down-conversion, resampling, clock recovery, CMA or MIMO CMA, frequency offset estimation (FOE), phase compensation, synchronization, and MRC.

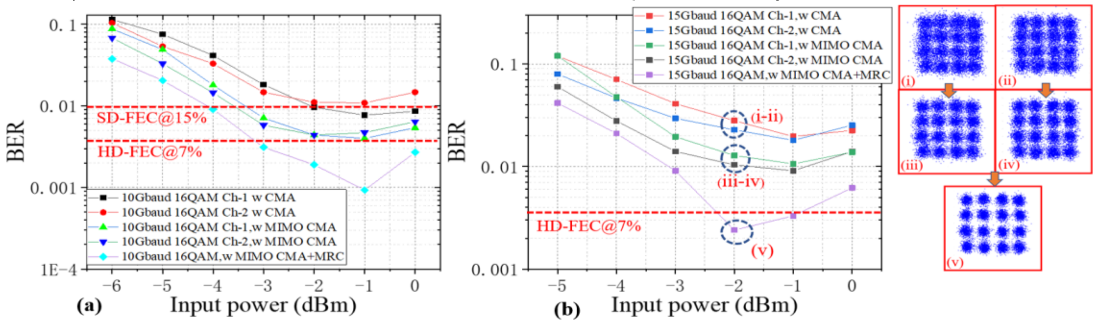

Fig.3: (a) BER of 10Gbaud16QAM signals vs. input power of PD; (b) BER of 15Gbaud16QAM signals vs. input power of PD.

Experimental Results and Discussions

The BER curves versus the input power of PD for 10 and 15Gbaud 16QAM signals are demonstrated in Fig.3(a) and (b), respectively. Because the PAs and LNAs are affected by the saturation effect, it can be seen that the BER curves depicted in Fig.3(a-b) all show a trend of first falling and then rising. With CMA in the DSP, the BER performance of Ch-1 and Ch-2 is not good. In order to improve the performance of the system, we first use MIMO CMA to jointly process the received signals of Ch-1 and Ch-2 to obtain a more accurate estimate of the channel impulse response, which can effectively improve signal quality by compensating for channel impairments. With MIMO CMA in the DSP, it can bring 1.5 dB optical power budget improvement under the soft-decision forward error correction (SD-FEC) threshold of 15% for 10Gbaud 16QAM signals. In order to achieve maximum improvement in system performance, we adopt a joint MIMO CMA and MRC receiving technology to improve the SNR of our receivers so that the transmission system can support a higher data rate. It can be seen that the BER can be reduced below 3.8×10^{-3} corresponding to 7% hard-decision forward error correction (HD-FEC) overhead for 10 and 15Gbaud 16QAM signals. The inset(i-v) in Fig.3(b) shows the demodulated constellations of 15Gbaud 16QAM signals corresponding to different technical processing. Obviously, the constellation in inset(v) is clearer than the constellations in inset(i-iv). The joint MIMO CMA and MRC receiving technology has better performance improvement than MIMO CMA or CMA.

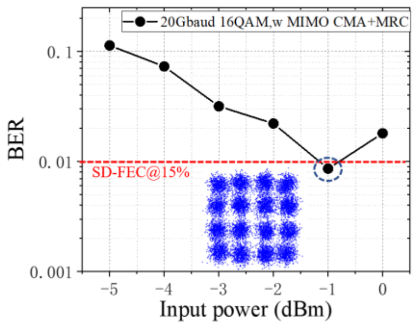

Fig.4: BER of 20 Gbaud 16QAM signals with MIMO CMA and MRC technology.

Based on the above joint MIMO CMA and MRC receiving technology, we measure the BER performance of 20Gbaud 16QAM signals shown in Fig.4. With -1dBm input power of PDs, the BER is below 1×10^{-2} corresponding to 15% SD-FEC overhead. Therefore, the data rate of the photonics-aided SIMO system is 20×4=80-Gbps. If removing the 15% SD-FEC overhead, the maximum net rate is 20×4/(1+15%)=70-Gbps.

Conclusions

In this paper, we have demonstrated a photonics-aided SIMO MMW delivery system employing our proposed MIMO CMA and MRC receiving technology, which shows great performance on compensating for channel impairments and improving signal quality. Through rigorous outdoor field experimental testing, we have successfully demonstrated the delivery of 80-Gbps 16QAM signals over a wireless distance of 4600 meters.

Acknowledgements

This work was partially supported by the NNSF of China with 61720106015 and 62127802.

References

[1] S. Ishimura, T. Fukui, R. Tanomura, G. Soma, Y. Nakano, and T. Tanemura, “64-QAM Self-Coherent Transmission Using Symmetric Silicon Photonic Stokes-Vector Receiver,” in Optical Fiber Communication Conference, M4J.6, 2022.

[2] K. Powell, A. Shams-Ansari, S. Desai, M. Austin, J. Deng, N. Sinclair and X. Yi. “High-Q suspended optical resonators in 3C silicon carbide obtained by thermal annealing,” Optics express, vol. 28, no. 4, pp.4938-4949, 2020.

[3] Z. Cao, X. Zhang, G. Osnabrugge, J. Li, I. Vellekoop and A. Koonen. (2019). “Reconfigurable beam system for non-line-of-sight free-space optical communication”. Light: Science & Applications. vol. 8, no. 1, pp.1-9, 2019.

[4] A. Delmade, E. Martin, C. Browning and L. Barry, “5G Millimeter-Wave Analog RoF System employing Optical Injection Locking and Direct Modulation of DFB Laser,” in Optical Fiber Communication Conference, W4C.7, 2022.

[5] G. Carpintero, Y. Yoshida, and J. Azaña, “Editorial Special Issue on Microwave Photonics,” Journal of Lightwave Technology. vol. 39, no. 24, pp. 7549-7550, 2021.

[6] X. Li, J. Xiao, and J. Yu, “Long-Distance Wireless mm-Wave Signal Delivery at W-Band,” Journal of Lightwave Technology. vol. 34, no. 2, pp. 661-668, 2016.

[7] A. Kanno, K. Inagaki, I. Morohashi, T. Sakamoto, T. Kuri, I. Hosako, T. Kawanishi, Y. Yoshida, and K. Kitayama. “20-Gb/s QPSK W-band (75-110GHz) wireless link in free space using radio-over-fiber technique,” IEICE Electronics Express, vol. 8, no. 8, pp. 612-617, 2011.

[8] X. Pang, A. Caballero, A. Dogadaev, V. Arlunno; L. Deng; R. Borkowski; J. S. Pedersen; D. Zibar, X. Yu, and I. T. Monroy. “25 Gbit/s QPSK Hybrid Fiber-Wireless Transmission in the W-Band (75–110 GHz) With Remote Antenna Unit for In-Building Wireless Networks," IEEE Photonics Journal, vol. 4, no. 3, pp. 691-698, 2012.

[9] R. Puerta, S. Rommel, J. J. V. Olmos, and I. T. Monroy, “Optically Generated Single Side-Band Radio-over-Fiber Transmission of 60Gbit/s over 50m at W-Band,” in Optical Fiber Communication Conference, M3E.4, 2017.

[10] W. Li, J. Yu, Y. Wang, F. Wang, B. Zhu, L. Zhao, W. Zhou, J. Yu, and F. Zhao. “OFDM-PS-256QAM signal delivery at 47.45 Gb/s over 4.6-kilometers wireless distance at the W band,” Optics letters, vol. 47, no. 16, pp. 4072-4075, 2022.

[11] W. Li, J Yu, J. Ding, X. Ji, Y. Wang, K. Wang, W. Zhou, F. Zhao, J. Yu, C. Wang, C. Li, and Z. Zhong. “23.1-Gb/s 135-GHz Wireless Transmission Over 4.6-Km and Effect of Rain Attenuation,” in IEEE Transactions on Microwave Theory and Techniques, doi: 10.1109/TMTT.2023.3267547.

[12] D. Godard. “Self-recovering equalization and carrier tracking in two-dimensional data communication systems,” In IEEE Transactions on communications, vol. 28, no. 11, pp. 1867-1875, 1980.

[13] J. Zhang, J. Yu, N. Chi, Z. Dong, X. Li and G. K. Chang, “Multichannel 120-Gb/s Data Transmission Over 2×2 MIMO Fiber-Wireless Link at W-Band,” in IEEE Photonics Technology Letters, vol. 25, no. 8, pp. 780-783, 2013.

[14] S. J. Savory, “Digital filters for coherent optical receivers,” Opt. Express, vol. 16, no. 2, pp. 804–817, 2008.

[15] A. J. Goldsmith, Wireless Communications, Cambridge University Press, New York, 2005.